Development 129, 1131-1141 (2002)
Printed in Great Britain © The Company of Biologists Limited 2002
DEV0399

MAX1 and *MAX2* control shoot lateral branching in *Arabidopsis*

Petra Stirnberg, Karin van de Sande and H. M. Ottoline Leyser

Department of Biology, University of York, PO Box 373, York YO10 5YW, UK
*Author for correspondence (e-mail: hmol1@york.ac.uk)

Accepted 4 December 2001

SUMMARY

Plant shoots elaborate their adult form by selective control over the growth of both their primary shoot apical meristem and their axillary shoot meristems. We describe recessive mutations at two loci in *Arabidopsis*, *MAX1* and *MAX2*, that affect the selective repression of axillary shoots. All the first order (but not higher order) axillary shoots initiated by mutant plants remain active, resulting in bushier shoots than those of wild type. In vegetative plants where axillary shoots develop in a basal to apical sequence, the mutations do not clearly alter node distance, from the shoot apex, at which axillary shoot meristems initiate but shorten the distance at which the first axillary leaf primordium is produced by the axillary shoot meristem. A small number of mutant axillary shoot meristems is enlarged and, later in development, a low proportion of mutant lateral shoots is fasciated. Together, this suggests that *MAX1* and *MAX2* do not control the timing of axillary meristem initiation but repress primordia formation by the axillary meristem. In addition to shoot branching, mutations at both loci affect leaf shape. The mutations at *MAX2* cause increased hypocotyl and petiole elongation in light-grown seedlings. Positional cloning identifies MAX2 as a member of the F-box leucine-rich repeat family of proteins. MAX2 is identical to ORE9, a proposed regulator of leaf senescence (Woo, H. R., Chung, K. M., Park, J.-H., Oh, S. A., Ahn, T., Hong, S. H., Jang, S. K. and Nam, H. G. (2001) *Plant Cell* 13, 1779-1790). Our results suggest that selective repression of axillary shoots involves ubiquitin-mediated degradation of as yet unidentified proteins that activate axillary growth.

Key words: Axillary shoot meristem, Hypocotyl elongation, Leaf shape, F-box leucine-rich repeat protein, ORE9, MAX, Ubiquitin-mediated proteolysis, *Arabidopsis thaliana*

INTRODUCTION

Branching plays an important role in the elaboration of plant adult body plans. The shoots of higher plants are characterised by axillary branching, where branches develop from axillary shoot meristems located between a leaf and the shoot axis. Variation of the pattern of axillary shoot meristem initiation and activity contributes to the diversity of plant shoot architecture and allows individuals to adapt their shoot morphology to the environment (Sussex and Kerk, 2001). Axillary shoot meristems may develop from cells at the base of the subtending leaf, or from cells in the shoot axis just above the subtending leaf; they may initiate at the same time as the subtending leaf, or with some delay when the subtending leaf is already differentiating (Evans and Barton, 1997). Once initiated, axillary shoot meristems may either develop into branches instantaneously, or they may develop into an axillary bud in which growth arrests after a few axillary leaf primordia have formed. Axillary shoots may also cycle repeatedly between growth and arrest (Stafstrom and Sussex, 1992).

The control of axillary shoot growth is poorly understood. One focus of research has been the control by plant hormones, mainly auxin and cytokinins. This work (reviewed by Cline, 1994; Tamas, 1995), points to auxin as an inhibitory long distance signal produced in growing shoot apices and transported basipetally, but unlikely to act in the axillary shoot itself. Cytokinins, transported acropetally from the root, may act as activators directly within the axillary shoot.

Mutants that specifically lack the ability to control growth of some or all of their axillary shoot meristems provide a means of investigating the genes involved in branching control. Characterisation of the *Arabidopsis supershoot*/*bushy* mutants, which branch excessively and initiate multiple axillary shoots per node, identified a member of the cytochrome P450 gene family as a common element of control over both axillary meristem initiation and growth (Reintanz et al., 2001; Tantikanjana et al., 2001). In contrast, mutations at the *teosinte branched1* (*tb1*) locus in maize affect axillary shoot growth but not initiation. *tb1* loss-of-function mutants produce elongated branches ending in tassels, whilst wild-type axillary shoots are short and terminate in ears (Doebley et al., 1995). The *TB1* gene may function as a transcriptional regulator and is expressed in axillary shoots (Doebley et al., 1997). The effects of the *tb1* mutation on both axillary shoot growth and morphology indicate that *TB1* not only acts in growth repression but in fate determination of lateral shoots.

Mutations at three *DAD* (*Decreased Apical Dominance*) loci in petunia and at five *RMS* (*Ramosus*) loci in pea (reviewed by Napoli et al., 1999) result in lack of axillary shoot repression without affecting axillary shoot morphology. Although these genes have not yet been cloned, important clues about their action in branching control have come from systematic mutant

characterisation, including grafting studies and hormone analysis. *RMS* and *DAD* loci can be grouped according to whether their action is restricted to the shoot or whether they affect signalling between root and shoot, which appears to be important in branching control. Although auxin and cytokinin levels or transport are altered in some of the *rms* mutants, the changes are opposite to those predicted to cause increased branching and hence may reflect compensatory changes due to the increased branching. This does not exclude a role of auxin and cytokinin, but points to the existence of at least one other signal controlling branching, whose action or perception is affected by the *rms* mutations (Napoli et al., 1999). This signal likely interacts with auxin, because lateral outgrowth from decapitated *rms* mutant shoots is insensitive to inhibition by exogenous auxin, but when *rms* shoots are grafted onto wild-type roots, their auxin responsiveness is restored (Beveridge et al., 2000).

Here we describe mutations at two loci, *MAX1* and *MAX2*, in *Arabidopsis*. Like the mutations at the *RMS* and *DAD* loci, they reduce the repression of axillary growth and have few pleiotropic effects unrelated to branching. Cloning of the *MAX2* gene points to a role for ubiquitin-mediated protein degradation in axillary growth repression.

MATERIALS AND METHODS

Plant growth

For morphometric analysis of mature plants (Fig. 2, Fig. 5; Table 2 experiment I) seeds were sown onto F2 compost treated with the systemic insecticide Intercept 70WG (both from Levington Horticulture, Ipswich, UK) in shallow trays consisting of individual 4×4 cm pots (P40, Cookson Plantpak, Maldon, UK), with several seeds per pot. After 3 days cold treatment at 4°C, trays were transferred to a greenhouse with 16-hour supplementary lighting at 100 μmol/m^2/second, mean temperature 20°C, range 16-28°C. Plants were thinned to one per pot after germination and watered with tap water.

For analysis of lateral shoot growth by dissection and by microscopy (Fig. 3, Fig. 4; Table 2 experiment II), for scanning electron microscopy (SEM) of axillary shoots (Fig. 6, Fig. 7) and for leaf measurements (Table 3), seeds were cold-treated at 4°C in tap water for 3 days, and sown onto F2 compost either in 4×4 cm individual pot trays (later, thinned to one per pot), or in shallow trays (for SEM, 1 seed per 2.5 cm^2). Plants were grown at 21°C at a light intensity of 200 μmol/m^2/second in either 8-hour (short) or 16-hour (long) photoperiods, and watered with tap water. Plants kept in short photoperiods over a prolonged time were regularly watered with a solution containing mineral nutrients (see Wilson et al., 1990).

For analysis of hypocotyl growth (Fig. 8), seeds were sown onto Intercept-treated F2 compost in 4×4 cm pots at a density of 20 per pot, cold-treated in the dark at 4°C for 3 days, exposed to light for 8 hours and then incubated for 6 days at 21°C either in the dark, or in a 16-hour photoperiod at two different light intensities of 70 (high) or 10 (low) μmol/m^2/second from white fluorescent tubes.

Microscopy

For analysis of the early stages of axillary shoot development (Fig. 4), shoots were fixed, embedded in wax, sectioned and stained as previously described (Stirnberg et al., 1999), except that 4% formaldehyde was used as fixative.

For light microscopy of normal and fasciated lateral shoots (Fig. 5), stem pieces were fixed as above and embedded in Technovit (Heraeus Kulzer GmbH, Wehrheim, Germany). 6 μm transverse sections were cut with disposable metal knives, affixed to microscope slides, and stained with 1% Toluidine Blue in 1% disodium tetraborate solution.

For scanning electron microscopy (Fig. 6), shoots were fixed in formalin-acetic acid-ethanol, then washed and dissected in 70% ethanol such that only the cotyledons and the oldest two leaves with their associated axillary shoots remained. After further dehydration in a graded ethanol series, critical-point drying, mounting on aluminium stubs and coating with gold, specimens were examined in a Hitachi S2400 scanning electron microscope at a voltage of 8 kV.

Mutants and initial mapping

max1-1, induced in the genetic background Enkheim-2 (En-2), corresponds to line V367 from the Arabidopsis Information Service (AIS) collection by A. R. Kranz and was provided by the NASC (stock number N754). *max1-1* was introduced into the Columbia (Col) genetic background by seven backcrosses, without noticeable changes in phenotypic expression. For characterisation, we used *max1-1* lines selected after at least three backcrosses into the Col background, and Col as control. *max2-1* and *max2-2* were isolated from independent M_2 bulks in a screen of 20,000 M_2 plants for altered shoot branching. The M_2 resulted from an ethyl methane sulphonate (EMS) mutagenesis of 50,000 Columbia (Col) ecotype seeds (0.3% EMS, 11 hours). For mapping, *max1-1* was outcrossed to the Col ecotype and *max2-1* to the Landsberg *erecta* (L*er*) ecotype. Mutant F_2 individuals were genotyped for SSLP (Bell and Ecker, 1994) or CAPS (Konieczny and Ausubel, 1993) molecular markers polymorphic between En-2 and Col for *MAX1* and between Col and L*er* for *MAX2*.

Cloning of *MAX2*

We extended the mapping population and found that chromosome 2 markers m429 and BIO2, which were closely linked to *MAX2* (Table1), flanked the gene. 1300 mutant F_2 individuals were screened for recombination between *MAX2* and these markers. Recombinants were then genotyped for new CAPS markers, developed from the published sequence, in the interval between BIO2 and m429. This delimited *MAX2* to a 57 kb region between two markers situated on overlapping BAC clones F14N22 and F7D19. Marker F14N22-L is a Tru1I polymorphism in a 2363 bp PCR product amplified with primers 5′-TTTCCACTCTTCCTTCTACC-3′ and 5′-AGAGGG-ATAGGTTGATTTTG-3′. F7D19-H is a *Hae*III polymorphism in a 2248 bp PCR product amplified with primers 5′-CAGGATG-TTCAACTAACCAG-3′ and 5′-GTCTTTGTTGGGAGGTAGTC-3′. For mutant rescue, gel-purified restriction fragments from BAC clones F14N22 and F7D19 were ligated into the plant transformation vector pCAMBIA-2300 (GenBank accession no. AF234315), and transformed into *E. coli* (Sambrook et al., 1989). Purified *E. coli* plasmids were electroporated into *Agrobacterium tumefaciens* GV3101, and transformed strains were used to transform *max2-1* mutant plants by floral dipping (Clough and Bent, 1998). Rescue of the mutant phenotype in transgenic T_1 progeny was first obtained with a 9329 bp *Nhe*I fragment of F14N22 (clone a in Fig. 9A, bp 47832-57160 of accession AC007087) which contained only two predicted genes (F14N22.11 and F14N22.10) from the interval delimited by markers H and L. Two derivative clones were produced, in which terminal deletions from either side of the *Nhe*I fragment extended into the predicted coding region of either F14N22.10 or F14N22.11 from the 5′ end. *max2-1* was only rescued with the derivative clone in which F14N22.11 and its upstream region was intact (clone b in Fig. 9A, bp 47832-55351 of AC007087). For allele sequencing, two PCR products covering the F14N22.11 coding region were amplified from Col, *max2-1* and *max2-2* DNA extracts, gel-purified and sequenced by the fluorescent chain termination procedure (DNA Sequencing Facility, Department of Biochemistry, Oxford University), using internal primers.

RESULTS

max1 and *max2* mutants show enhanced shoot branching

In order to identify genes that control lateral branching in *Arabidopsis* shoots, we screened mutagenised populations. In addition, we examined lines from mutant collections whose description suggested that shoot branching was affected. Line V367 from the AIS mutant collection was described as forming "multiple flowering stems" (http://nasc.nott.ac.uk/catalogue.html). Enhanced development of the axillary shoots of rosette leaves in V367 compared to the corresponding wild-type En-2 was obvious early after the plants started to bolt and flower (Fig. 1A). At maturity, V367 had more lateral inflorescences than wild type (Fig. 1B). This phenotype was due to a recessive mutation (data not shown), which we renamed *max1-1* because it causes more axillary growth.

Two independent lines whose branching phenotype closely resembled *max1-1* were found in an EMS-mutagenised population of the Col ecotype. Seedlings from these lines differed from both *max1-1* and the wild type by their elongated hypocotyls and cotyledonary petioles (Fig. 1C). Branching and seedling phenotypes cosegregated and were recessive, and the EMS-induced mutations were allelic to each other but not allelic to *max1-1* (data not shown). Both alleles of this new locus, *MAX2*, caused very similar phenotypes, and the *max2-1* allele was chosen for further characterisation. *MAX1* and *MAX2* map to two different regions on chromosome 2 (Table 1).

To investigate a possible interaction between *MAX1* and *MAX2* in branching control, the *max1-1 max2-1* double mutant was constructed. First, we selected individuals homozygous for *max1-1* (normal hypocotyl, bushy shoot) in the F_2 from an intercross. Their individual F_3 progeny were then screened for segregation of double mutants showing the *max2-1* elongated hypocotyl phenotype.

First order branching is enhanced to the same extent in *max1* and *max2* mutant and double mutant shoots

In order to determine the effects of mutation at *MAX1* and *MAX2* on shoot architecture more precisely, wild type, mutant and double mutant plants were grown to maturity and their shoots examined (Fig. 2). *max1-1* and *max2-1* shoots were shorter than wild type, as indicated by the length of the primary inflorescence (Fig. 2A). Wild type and mutants produced similar numbers of vegetative, leaf-bearing nodes before floral transition (Fig. 2B). All these nodes have the potential to form a first order lateral inflorescence. However, in the wild type, only 39% of nodes produced a first-order branch, compared to 77% in *max1-1*, 76% in *max2-1* and 82% in the double mutant. This was due to differences in the proportion of rosette nodes producing a branch, whilst all the leaf-bearing nodes on the elongated primary inflorescence (the cauline nodes) produced a lateral branch in all genotypes (Fig. 2C). To quantify higher order branching, the ratio of the total number of branches (first and higher order) divided by the number of first-order branches was calculated for each shoot. The mutants did not differ significantly from the wild type in this ratio (data not shown). We also compared shoot growth in wild type and the mutants in terms of total fresh weight (FW) and FW distribution between the primary shoot (i.e. primary inflorescence and primary leaves) and the branches. We did not observe consistent differences between mutant and wild-type total shoot FW (data not shown). Furthermore, the proportion of lateral shoot FW per total shoot FW was similar for all genotypes (Fig. 2D). Thus, although *max1-1* and *max2-1* promoted outgrowth of a higher number of first order lateral branches, this had little effect on overall resource allocation between primary shoot axis and lateral shoots. Shoot architecture of the *max1-1 max2-1* double mutant was indistinguishable from that of the single mutants (Fig. 2A-D). All produced similar numbers of first-order lateral branches. The combination of both mutations did not have any additional effects on higher-order branching or on the FW distribution between primary shoot and the branches.

Table 1. Linkage analysis of *max1-1* and *max2-1*

Marker	Chromosome 2 position (section number of the complete sequence)	Chromosomes scored: MAX1* Total	MAX1* Recombinant	MAX2† Total	MAX2† Recombinant
ER	147	160	1	–	–
nga361	175	160	15	112	8
nga168	210	–	–	112	4
m429	211	–	–	110	3
BIO2	235	–	–	112	0

*of *max1-1* mutant F_2 individuals from an outcross of *max1-1* to the Col ecotype.

†of *max2-1* mutant F_2 individuals from an outcross of *max2-1* to the L*er* ecotype.

First order branching is enhanced at both vegetative and reproductive stages in *max1* and *max2* mutants

The timing and extent of axillary shoot growth depends on node position along the shoot axis, often resulting in a characteristic apical-basal pattern. *Arabidopsis* wild type shows two distinct patterns of lateral shoot development, which depend on the developmental stage (Hempel and Feldman, 1994; Grbić and Bleecker, 1996; Stirnberg et al., 1999). During the vegetative phase, axillary shoot meristems initiate in the axils of leaf primordia at some distance from the primary shoot apical meristem, and axillary shoot development progresses in parallel with development of the subtending leaf. This results in an acropetal progression of vegetative axillary shoot development. The second pattern, characteristic for the reproductive phase, is a basipetal progression of outgrowth of lateral inflorescences, which originate from axillary shoot meristems that arise even in the axils of the youngest leaf primordia in close proximity to the primary shoot apical meristem. In order to study the effect of *max1-1* and *max2-1* on these patterns of lateral shoot development, we determined the phyllotactic sequence of wild-type and mutant shoots, dissected the leaves with their associated axillary shoots from the shoot axis and recorded axillary shoot growth at consecutive node positions. *Arabidopsis* axillary shoots are connected to their subtending leaves as they originate from cells at the leaf base (Stirnberg et al., 1999; Long and Barton, 2000).

The growth of vegetative axillary buds developing in the acropetal wave was studied using plants grown in short photoperiods in order to prolong their vegetative phase. Five

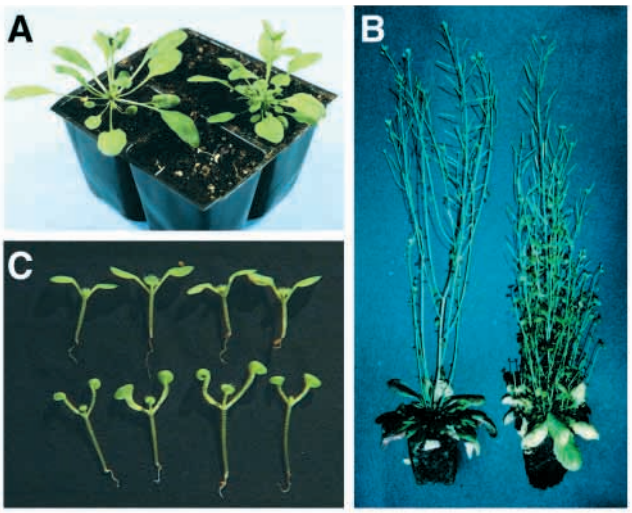

Fig. 1. Phenotypes of the *max* mutants. (A) Wild type (En-2, left) and *max1-1* (V367, right) soon after floral transition. (B) Wild type (Col, left) and *max1-1* (backcross 3 into Col, right) at maturity. (C) Wild-type (top) and *max2-1* (bottom) light-grown seedlings.

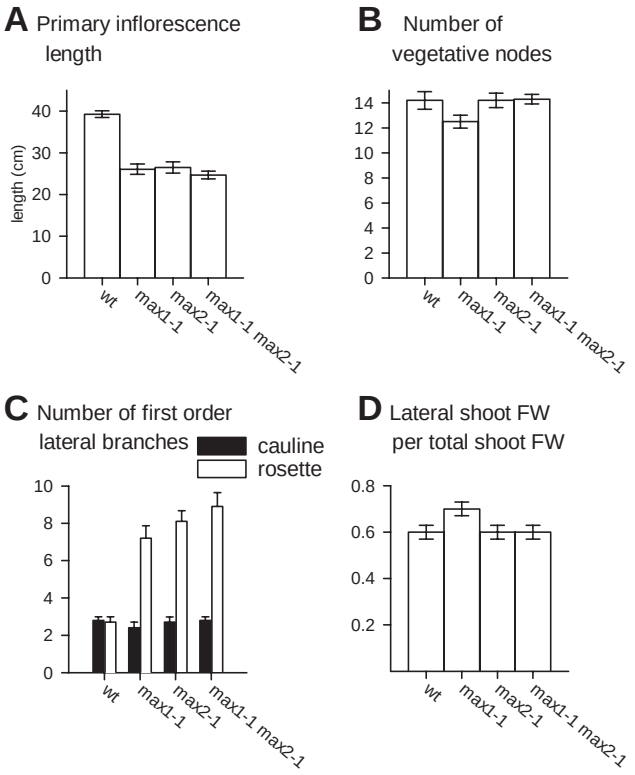

Fig. 2. Growth and lateral branching of wild-type (wt), *max1-1*, *max2-1* and *max1-1 max2-1* double mutant shoots. Plants were analysed near maturity, when flower production of the primary inflorescence had ceased (after 45-46 days of growth). (A) Length of the primary inflorescence. (B) Number of vegetative, leaf-bearing nodes on the primary shoot axis. (C) Number of first order lateral branches of at least 0.5 cm length, from nodes in the rosette and from cauline nodes on the primary inflorescence. (D) Fresh weight (FW) of the lateral shoot branches expressed as a proportion of the total shoot FW. (A-D) Means and 95% confidence intervals of the means are shown, n=17-18.

comparisons between one wild-type, one *max1-1* and one *max2-1* shoot were made between the 48th and 54th day of growth. One representative comparison is shown in Fig. 3A. In the wild type, the dissected leaves subtended axillary buds that, with very few exceptions, were uniform in size and so small that they are not visible at the magnification used. In the mutants, the youngest of the dissected leaves subtended buds that were only slightly larger than wild type, but the difference both in bud size and in the number of expanding axillary leaves increased between wild-type and mutant buds subtended by progressively older leaves.

The effect of *max1-1* and *max2-1* on the basipetal wave of outgrowth of inflorescence branches was investigated using plants grown in long photoperiods. The date of bolting, i.e. visible internode elongation of the primary inflorescence, was noted for each individual and shoots were dissected 9 days later (representative shoots in Fig. 3B). Mean lateral inflorescence lengths for consecutive node positions, starting from the most apical leaf-bearing node and proceeding basally are shown in Fig. 3C. In the wild type, mean lateral inflorescence lengths for the four most apical nodes were similar. On average, these represent the lateral inflorescences at the cauline nodes, as the mean number of cauline nodes was four. Further basal, into the rosette, mean inflorescence length progressively decreased over about four nodes. More basal rosette nodes carried visible axillary shoots but did not carry elongating lateral inflorescences. In mutant plants, lateral inflorescences were found at all node positions along the shoot axis. The pattern of lateral growth in the apical part of mutant shoots resembled that of the wild type, with about four apical leaves subtending lateral inflorescences of similar length and inflorescence length declining progressively at more basal positions. However, at apical node positions, mutant inflorescences were shorter than wild type; further basal they were longer, and the wave of elongating inflorescences extended further down into the rosette. At the most basal nodes, mutant lateral inflorescences were slightly longer again than the nodes in the middle of the rosette. The axillary buds giving rise to these basal inflorescences likely developed during vegetative growth and both their vegetative development (number and size of axillary leaves, Fig. 3B) and inflorescence length (Fig. 3C) conformed to an acropetal pattern.

In summary, *max1-1* and *max2-1* did not interfere with the growth-phase-characteristic patterns of lateral development. However, they affected the extent of axillary shoot growth in both patterns. Node positions, at which wild-type axillary shoots were very small, supported much more developed axillary shoots in the mutants. However, at least in the reproductive phase of the mutant shoots, the enhanced growth in these positions appeared to be compensated for by reduced growth in others, where the wild-type lateral shoots were more advanced.

The timing of axillary meristem formation is not altered in *max1* and *max2* mutant shoots

Mutant axillary buds are further developed than those of wild type at many node positions. This could be because they initiate earlier, or because of an increased rate of growth after initiation. To distinguish between these possibilities, we

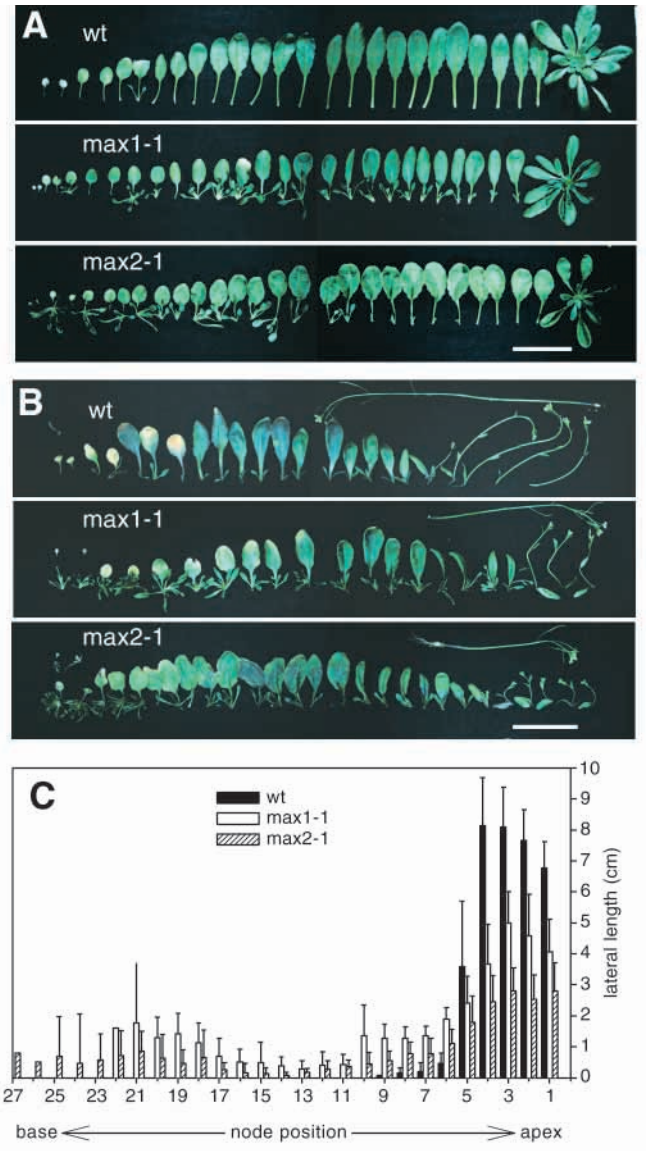

Fig. 3. Lateral shoot development at consecutive node positions of wild-type (wt), *max1-1* and *max2-1* shoots. (A,B) Leaves and associated axillary shoots dissected from the shoot axis and laid out in the order of emergence, oldest leaf to the left. Scale bar: 5 cm. (A) Vegetative shoots after 52 days of growth in short photoperiods. The oldest 25 leaves and their axillary shoots have been dissected from the shoot axis. The remaining apical parts of the shoots are shown at the right. (B) Flowering shoots grown in long photoperiods, 9 days after the primary inflorescence started elongating. All the leaves and their axillary shoots were dissected from the shoot axis, the remaining primary inflorescences are shown at the top right. (C) Mean lateral inflorescence lengths and 95% confidence intervals of the means at consecutive node positions, conditions as in B. For nodes carrying a vegetative axillary shoot, lateral inflorescence length was scored as 0. Number of shoots analysed: wt *n*=12; *max1-1*, *max2-1* *n*=7. The numbers of leaf-bearing nodes along the primary shoot axis ranged between 18 and 23 for wt, 19 and 23 for *max1-1* and 19 and 27 for *max2-1*.

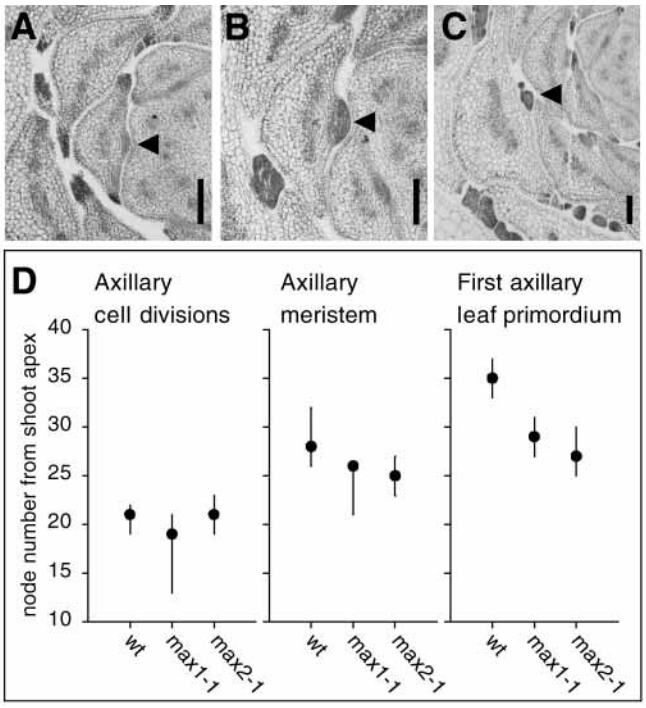

Fig. 4. Timing of axillary shoot initiation in wild type, *max1-1* and *max2-1*. Series of transverse sections of individual shoots grown in short photoperiods for 36 days were prepared and axillary shoot development at consecutive node positions was scored into three stages. (A-C) Sections from wild-type shoots, showing the developing axillary shoots (arrowheads) illustrating the stages scored. Scale bars: 100 μm. (A) Stage 1: axillary cell divisions at the base of a developing leaf, visible above the insertion point into the shoot axis. (B) Stage 2: axillary meristem bulging out from the base of the subtending leaf; the angle with the adaxial side of the leaf is at least 45°. (C) Stage 3: first axillary leaf primordium separated from the axillary shoot meristem by a cleft. (D) Node number from the shoot apex at which the three early stages of axillary shoot development first occurred in wild type (wt), *max1-1* and *max2-1*. Circles represent the median, bars extend between the minimum and maximum observed node number of first occurrence of each stage. Number of shoots examined: wild type *n*=9; *max1-1*, *max2-1*, *n*=11.

compared the early stages of axillary shoot development for wild-type and mutant plants grown in short photoperiods, where axillary shoots initiate and develop acropetally. 36-day-old shoots were fixed and embedded, and a series of transverse sections prepared from each shoot. For each series, the leaf primordia were numbered in order of increasing age. Axillary shoot development at each leaf position was then classified into three stages (Fig. 4A-C): stage 1 – axillary cell divisions; stage 2 – appearance of the axillary meristem; stage 3 – formation of the first axillary leaf primordium. Fig. 4D summarises at which node these stages were first observed. In the wild type, the axillary cell division stage was first observed at 19-22 nodes distant from the apex, with median 21. The distances for first appearance of the axillary meristem ranged between 26 and 32 nodes (median 28) and for first axillary leaf primordium formation between 33 and 37 nodes (median 35) from the apex. Although axillary cell divisions were seen closer to the apex in some *max1-1* individuals and axillary meristems were seen closer to the apex in some *max1-1* and some *max2-1* individuals, the ranges of node positions at which stages 1 and 2 first occur still overlapped for all three genotypes. Thus the mutations do not clearly affect the timing of axillary meristem

formation. In contrast, the ranges of node positions for the first occurrence of stage 3 in the mutants did not overlap with that in the wild type. All the *max1-1* and *max2-1* individuals produced the first axillary leaf primordium at a shorter node distance from the apex than the wild-type individuals. Therefore, the advanced development of mutant vegetative axillary shoots appears to be due to increased growth subsequent to meristem initiation.

Axillary shoots of *max1* and *max2* mutant plants are sometimes fasciated

Loss of repression of axillary growth is a trait shown by all *max1-1* and *max2-1* mutant individuals. When dissecting mutant and double mutant shoots in order to analyse shoot architecture, we noted two unusual types of axillary shoot development in some mutant individuals: first, two lateral inflorescences, of about equal strength, growing out from one axil (Fig. 5A); second, fasciated lateral inflorescences with flattened, sometimes bifurcating stems and with irregular phyllotaxy (Fig. 5B-D). Transverse sectioning showed that these fasciated laterals had more vascular bundles, but tissue organisation appeared normal otherwise (Fig. 5E-H). We did not observe fasciation of the primary inflorescence in the mutants. Both the twin and the fasciated lateral inflorescences were found in the axils of older rosette leaves close to the base, at frequencies summarised in Table 2. The frequency of individuals with a fasciated lateral shoot was similar for *max1-1* and *max2-1* (between 11 and 17%), but was clearly increased in the *max1-1 max2-1* double mutant (35%). The occurrence of mutant individuals with twin lateral inflorescences varied considerably between two experiments. In experiment I, which included the double mutant, it was very rare. Only some *max2-1* individuals with twin inflorescences were detected, and there was no evidence for an increased occurrence of twin laterals in *max1-1 max2-1*.

In order to investigate the origin of the abnormal laterals we compared early stages of wild-type and mutant axillary shoots subtended by the oldest pair of leaves by scanning electron microscopy. Fig. 6A-C shows three successive stages of wild-type axillary shoots. First, the adaxial side of the leaf base displays a semicircular zone of very small epidermal cells (Fig. 6A). Second, the semicircular zone bulges out to form the axillary shoot meristem (Fig. 6B). Third, the first pair of axillary leaf primordia is typically initiated at two opposite positions on the axillary shoot meristem and at right angles to the subtending leaf (Fig. 6C). In most mutant axils, developing lateral shoots were similar to those found in the wild type. However, some axillary shoots of *max1-1* (Fig. 6E-G) and *max2-1* (Fig. 6I-K) appeared to have diverged from normal development, with semicircular meristematic zones and axillary shoot meristems larger than wild type. Some mutant axillary meristems initiated leaf primordia in random positions. Such axillary buds might have developed into fasciated shoots. In order to quantify axillary meristem size in wild type and mutants, the area occupied by the meristematic cells was measured for all wild type and mutant axils corresponding to the stages in Fig. 6A,B, i.e. prior to axillary leaf primordium formation. The frequency distribution of the meristematic areas for the mutants extended to larger sizes than for the wild type (Fig. 7). In some axils of both wild type and mutants, we observed the development of an additional, accessory axillary shoot (Fig. 6D,H,L). Therefore, the appearance of twin lateral inflorescences in the mutants is likely due to their inability to repress axillary shoot growth rather than an increased capacity to initiate accessory shoot meristems.

Table 2. Frequency of individual plants with abnormal first order branches in the wild type, in *max1-1*, *max2-1* and in the *max1-1 max2-1* double mutant

	Genotype			
	Wild type	*max1-1*	*max2-1*	*max1-1 max2-1*
Experiment I				
Total	54	54	54	48
With fasciated branch	0	6 (11%)	6 (11%)	17 (35%)
With two branches from one axil	0	0 (0%)	3 (6%)	0 (0%)
Experiment II				
Total	55	28	36	–
With fasciated branch	0	3 (11%)	6 (17%)	–
With two branches from one axil	0	13 (46%)	12 (33%)	–

max1 and *max2* mutant plants have round leaves and the *max2* mutant has an elongated hypocotyl in the light

max1-1 and *max2-1* rosette leaves appeared rounder than wild type, with shorter petioles (Fig. 3A,B). As an example, Table 3 shows the dimensions of the 11th leaf, counting from the base, from plants grown in short photoperiods. Mutant leaves had a reduced area, their leaf length and petiole length was reduced, while leaf width was almost the same as wild type. Mutant leaf length/width ratios were lower than wild type.

Only *max2-1* but not *max1-1* affected seedling growth. *max2-1* hypocotyls were significantly longer than those of wild type in the light, but not in the dark (Fig. 1C, Fig. 8). Sometimes, the petioles of the cotyledons (Fig. 1C) and the juvenile leaves (data not shown) were also more elongated in light-grown *max2-1*. Thus, mutations at *MAX2* had opposite effects on the growth of the embryonic and juvenile compared to older leaves.

Map-based cloning of the *MAX2* gene

The *MAX2* gene was cloned by a map-based approach (Fig. 9A, Materials and Methods). The *MAX2*-containing region on chromosome 2 was delimited to a 57 kb interval flanked by two newly developed CAPS markers, F14N22-L and F7D19-H. Wild-type genomic fragments from this interval, subcloned from BAC clones, were then transformed into *max2-1*. The smallest fragment that rescued the mutant phenotype (clone b,

Table 3. Morphometry of the rosette leaf of node 11 (from the base) in wild-type, *max1-1* and *max2-1* plants

	Wild type*	*max1-1**	*max2-1**
Leaf area (cm^2)	3.74±0.66	2.20±0.40	2.64±0.47
Leaf length (cm)	5.49±0.37	3.50±0.24	3.67±0.37
Petiole length (cm)	2.07±0.09	1.26±0.06	1.31±0.15
Leaf width (cm)	1.65±0.14	1.42±0.12	1.55±0.16
Length/width ratio	3.33±0.12	2.46±0.13	2.38±0.06

*Mean±95% confidence interval of the mean for 6 leaves per genotype.

Fig. 9A) contained only one predicted gene from the mapping interval, F14.N22.11 (accession AC007087, bp 51282-53363), indicating that this was the *MAX2* gene. Fig. 9B shows the predicted F14N22.11 protein sequence. The published annotation predicted a single 45 bp intron that would have led to splicing out of the codons for amino acids 373-387. However, these codons are present on a published partial *Arabidopsis* cDNA identical to F14N22.11 (AV539757). Sequencing revealed that both *max2* mutant alleles had a single G to A base change in the F14N22.11 coding region. They predict an aspartate to asparagine amino acid change at position 581 for *max2-1* and a premature translation stop at position 585 for *max2-2* (Fig. 9B).

A motif search (http://smart.embl-heidelberg.de/) with the predicted MAX2 sequence indicated the presence of an N-terminal F-box domain, and three leucine-rich repeat (LRR) motifs (LRR 6,11,12 in Fig. 9B). This suggests that MAX2 is a member of the F-box LRR family of proteins that function in protein ubiquitination as substrate-recruiting subunits of the SCF-type ubiquitin E3 ligase complexes (Patton et al., 1998; Jackson et al., 2000). Fig. 9B shows that the predicted MAX2 protein contains repeats of the motif LxxLxL, with L (leucine) sometimes replaced by I (isoleucine). MAX2 deviates from a perfect LRR structure (Kobe and Deisenhofer, 1994), as the distance between the repeats varies.

MAX2 is identical to the *ORE9* gene (also in *Arabidopsis*), whose map-based cloning was reported recently (Woo et al., 2001). *ORE9* was defined by a single mutant allele, *ore9-1*, which delays the onset of in-planta and hormone-induced leaf senescence (Oh et al., 1997).

Database searches with the predicted MAX2 protein sequence revealed no close homolog in *Arabidopsis*. However, translated partial cDNA clones from other plant species (*Medicago truncatula*, cotton, soybean, potato, *Pinus taeda*) show high homology to MAX2 (50 to 80% amino acid identity). Fig. 9C shows an alignment of the predicted MAX2 F-box with those found in other characterised or predicted plant proteins. The predicted amino acid sequence of two *Medicago truncatula* ESTs (AL369069, BE325112) that likely represent the same mRNA shows 58% identity to MAX2 over the F-box. For F-box proteins from *Arabidopsis*, TIR1 (Ruegger et al., 1998), COI1 (Xie et al., 1998), ZTL (Somers et al., 2000) and UFO (Samach et al., 1999), amino acid identities to MAX2 over the F-box region range between 31 and 20%. The predicted MAX2 sequence matches 44% of the consensus residues derived from an alignment of F-box containing proteins from different organisms (Patton et al., 1998).

DISCUSSION

MAX1 and *MAX2* repress shoot lateral branching

The most striking phenotype of plants carrying mutations at *MAX1* or *MAX2* is the bushy appearance of their shoots. Our detailed analysis of branching in mutant shoots shows that the growth-phase-specific patterns of axillary shoot development were not altered. However, axillary growth repression was abolished at node positions that show little axillary growth in the wild type, both in vegetative and in reproductive shoots. This indicates common regulation of axillary shoot growth in both patterns. The loss of growth repression in *max1* and *max2* plants was confined to axillary shoots in specific positions. The outgrowth from first order and accessory axillary meristems at nodes in the rosette near the base of the shoot was enhanced. However, neither higher order branching, nor the outgrowth of accessory axillary shoots from nodes on the inflorescence was promoted.

The *max1* and *max2* alleles we studied had no clear effect on the timing of axillary meristem formation. Therefore, *MAX1* and *MAX2* appear specifically to control axillary growth rate after axillary meristem initiation, by regulating the rate of axillary leaf primordium formation and development. The sustained higher leaf initiation rate of *max1* and *max2* mutant axillary shoots must be accompanied by a higher cell production rate of the axillary shoot meristem. Overexpression of the G_1 cyclin D2 in tobacco has demonstrated that the rate of meristematic cell production controls the rate of leaf primordia formation and growth (Cockcroft et al., 2000). Therefore *MAX1* and *MAX2* might repress axillary growth by controlling the rate of cell production specifically in axillary shoot meristems. Increasing cell division rate by overexpression of cyclin D2 had no effect on meristem size in transgenic tobacco (Cockcroft et al., 2000). In contrast, *max1* and *max2* mutant plants occasionally produced enlarged axillary shoot meristems and fasciated lateral shoots. Again, this points to a role for *MAX1* and *MAX2* in balancing cell production and leaf primordia formation in axillary shoot meristems. Fasciation, specific to lateral shoots, as in *max1* and *max2*, has not been reported previously. In particular, other mutations affecting axillary growth repression do not appear to confer this phenotype.

Plants are able to adapt their body plan to the environment. One important aspect of this ability is the control over axillary shoot growth. First, selective promotion of branching at some nodes and repression at others may contribute to an optimal use of light. *max1* and *max2* mutant plants lack this selective control over first order branching. Second, plants concentrate growth in the main shoot apex at the expense of the branches under conditions where water, nutrient, or light are limited (Phillips, 1975; Cline, 1991). The FW mass distribution between the main shoot axis and the branches in *max1* and *max2* was not different from that in the wild type under normal growth conditions (Fig. 2A). However, under nitrogen starvation, mutant shoots had a significantly higher lateral / total FW ratio than the wild type, whilst total shoot FW was reduced to the same extent as in the wild type (P. S., unpublished). These observations suggest that *MAX1* and *MAX2* are necessary for optimal adaptation of shoot architecture to the environment.

The similarity of the branching phenotypes caused by the mutations in *MAX1* and *MAX2* raises the question of whether both genes act in a common pathway in branching control. Analysis of the *max1 max2* double mutant does not unequivocally answer this question. The phenotypic effects of combining *max1* and *max2* in the double mutant varied for different traits. With regard to first order lateral branching, and the occurrence of additional, accessory branches from rosette nodes, the double mutant was not significantly different from either single mutant. This is indicative of an action of both genes in a common pathway of branching control. However, as first order branching is nearly maximal in the single mutants,

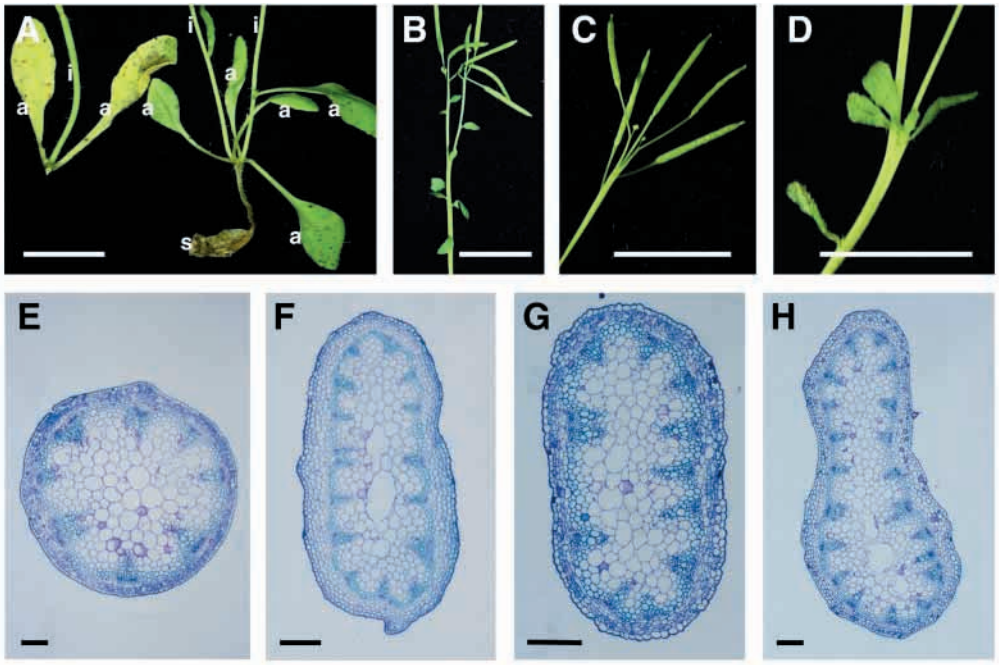

Fig. 5. Abnormal lateral branches observed in *max1-1*, *max2-1* and *max1-1 max2-1* double mutant shoots. (A) Lateral growth from one rosette leaf axil of wild type (left) and *max2-1* (right). There is a single lateral inflorescence in wild type and two lateral inflorescences in the mutant. s, leaf subtending the lateral shoot; a, axillary leaf; i, stem of lateral inflorescence. (B-D) Fasciated lateral inflorescences of (B) *max1-1*, (C) *max2-1*, (D) *max1-1 max2-1*. (E-H) Transverse sections of (E) a wild-type lateral inflorescence and (F) *max1-1*, (G) *max2-1* and (H) *max1-1 max2-1* fasciated lateral inflorescences. Scale bars: 1 cm (A-D); 100 μm (E-H).

one might argue that this prevented the detection of an additive effect in the double mutant, even if both genes acted independently. Indeed, for another trait, the frequency of individuals with fasciated shoots, the double mutant showed an enhanced phenotype compared to the single mutants. It is likely that both axillary shoot phenotypes, lack of growth repression and increased meristem size, have the same molecular basis. Axillary growth repression may be affected uniformly in all single and double mutant individuals because it is very sensitive to loss of *MAX1* or/and *MAX2* activity. In contrast, meristem size control may only be affected by more drastic loss of *MAX1* and *MAX2* function, which could result in the double mutant given that the *max1* and *max2* alleles we isolated were leaky. At present, it is unclear whether the *max2-1* allele, which we used to construct the double mutant and which is a missense mutation, causes complete or partial loss of gene function. The nature of the *max1-1* allele is not yet known. The EMS-mutagenised M_2 population we screened for branching mutants was relatively small. Isolation of additional, in particular, complete loss-of-function alleles at both loci is necessary to investigate further the interaction between *MAX1* and *MAX2*.

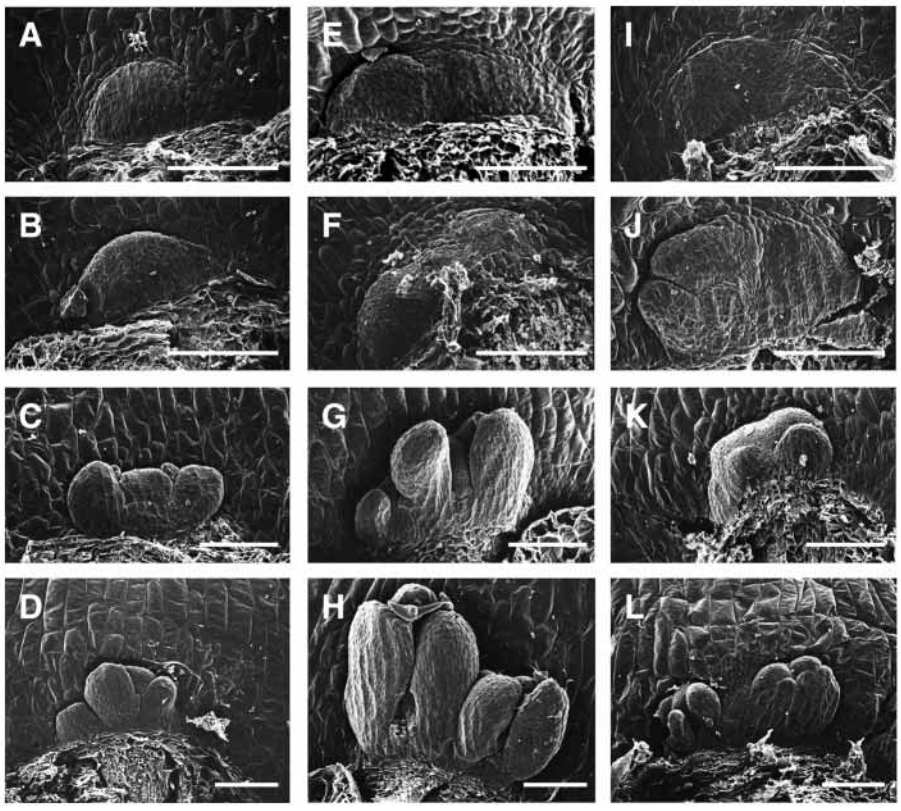

Fig. 6. Scanning electron micrographs of developing axillary shoots at the base of the oldest pair of leaves of wild type (A-D), *max1-1* (E-H) and *max2-1* (I-L). Plants were fixed after 14-16 days of growth in long photoperiods. The figure shows normal wild-type buds and mutant buds that appeared abnormal. Scale bars: 100 μm.
(A,E,I) Semicircular zone marks initiation of axillary shoot. The size increased in some mutant axils. (B,F,J) Axillary shoot meristem bulging out. The size increased in some mutant axils. (C,G,K) Formation of axillary leaf primordia. Two primordia form at opposite positions in the wild type, but the position can be random in the mutants. (D,H,L) Leaf bases with more than one axillary shoot meristem. One of the two axillary shoots is retarded in the wild type, but in the mutants both develop.

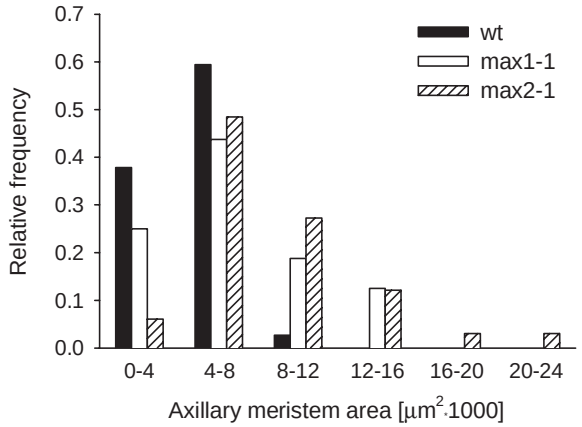

Fig. 7. Size of axillary meristems in the axils of the oldest two leaves of wild-type (wt), *max1-1* and *max2-1* plants analysed by scanning electron microscopy. The area occupied by axillary meristematic zones or axillary meristems prior to axillary leaf primordium formation was measured on scanning electron micrographs of individual leaf axils. Relative frequency distribution is shown. Number of measurements: wild type *n*=37, *max1-1 n*=16, *max2-1 n*=33.

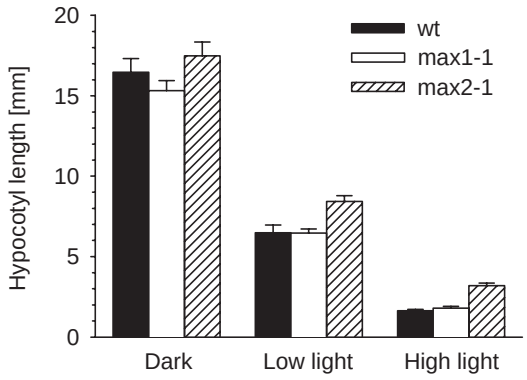

Fig. 8. Hypocotyl length of wild-type (wt), *max1-1* and *max2-1* seedlings after 6 days of growth in the dark, or at two different light intensities in a 16-hour photoperiod. Means and 95% confidence intervals of the means are shown, *n*=20-21.

MAX1 and *MAX2* are involved in other developmental processes

In addition to the enhanced branching, we noted a few other phenotypic effects of the mutations at the *MAX1* and the *MAX2* loci. Mutations at both loci affect leaf shape. The rounder shape of *max1* and *max2* leaves is due to a reduced leaf length. This resembles the leaflet phenotype reported for the branching mutants pea, *rms1*, *rms2* and *rms4* (Beveridge et al., 1996; Beveridge et al., 1997). The fact that mutations at several loci in *Arabidopsis* and pea affect branching and leaf development in a similar way suggests that these processes are linked.

Mutations at the *MAX2* locus affect seedling growth. *max2* hypocotyls were significantly longer than those of wild type in the light but not in the dark, suggesting that *MAX2* acts in light or circadian control of growth. Although mutations have been described that affect both hypocotyl growth and branching, they either cause an elongated hypocotyl and reduced branching, or a short hypocotyl and increased branching (Chory, 1993; Millar et al., 1994).

MAX2 is identical to the *ORE9* gene, a regulator of leaf senescence

Recent cloning of the *ORE9* locus of *Arabidopsis* (Woo et al., 2001), which is identical to *MAX2*, reveals an additional role for this gene in the regulation of leaf senescence. Leaves of the *ore9-1* mutant show a delayed onset of senescence, both in planta and when detached and subjected to senescence-inducing treatments (Oh et al., 1997). *ore9-1* is a nonsense mutation at position 327 of the protein (Woo et al., 2001), and therefore likely causes the most severe loss of function of the three known *ore9/max2* alleles. *ore9-1* shoots are bushy [see fig. 1 in Oh et al. (Oh et al., 1997)]. It is unlikely that enhanced branching is a secondary consequence of delayed leaf senescence in *ore9/max2* plants, as the difference in axillary leaf primordia formation between wild-type and *max2* shoots (Fig. 4) was detectable before the onset of leaf senescence in either genotype. Conversely, the mutations at the *RMS* branching loci in pea differ in their effects on leaf senescence (Beveridge, 2000), which indicates that delayed leaf senesce is not in general a consequence of increased axillary branching.

MAX2 encodes an F-box leucine-rich repeat protein

MAX2 is a member of the F-box LRR family. Members of this protein family function as subunits of the multiprotein SCF-type E3 ligases that polyubiquitinate proteins and thus target them for degradation by the 26S proteasome (Patton et al., 1998; Jackson et al., 2000). By mediating the degradation of cell division regulators, transcription factors and other proteins involved in signal transduction and environmental sensing, SCF complexes regulate a wide range of eukaryotic cellular processes (Craig and Tyers, 1999). F-box proteins confer substrate specificity to the SCF complex via their two distinct functional domains. The F-box domain binds to another subunit of the SCF, a member of the Skp1 protein family. The second domain, which may consist of LRR, or WD40 repeats, interacts with specific proteins to be polyubitquitinated by the SCF. Although some F-box proteins may function in processes other than SCF-mediated proteolysis (Kaplan et al., 1997; Russell et al., 1999; Clifford et al., 2000; Galan et al., 2001), this has not been reported for any members of the F-box LRR protein family. Therefore, MAX2 likely functions in SCF-mediated protein degradation.

Molecular cloning of mutant loci has provided insight into the processes that F-box proteins regulate in plants. TIR1 and COI1 are F-box LRR proteins that function in auxin and in jasmonate signalling, respectively (Ruegger et al., 1998; Xie et al., 1998). Amongst F-box proteins lacking LRR, UFO is required for normal growth and patterning of floral meristems (Samach et al., 1999; Zhao et al., 2001). Two related proteins, ZTL1 and FKF1, mediate light control of the circadian clock (Somers et al., 2000; Nelson et al., 2000). EID1 acts in phytochrome A-mediated light signalling (Dieterle et al., 2001). MAX2/ORE9 controls several, apparently unrelated processes at different stages of the plant's life cycle. It might perform these multiple functions by targeting different proteins for degradation, like some F-box proteins in yeast and humans (Patton et al., 1998; Tyers and Jorgensen, 2000).

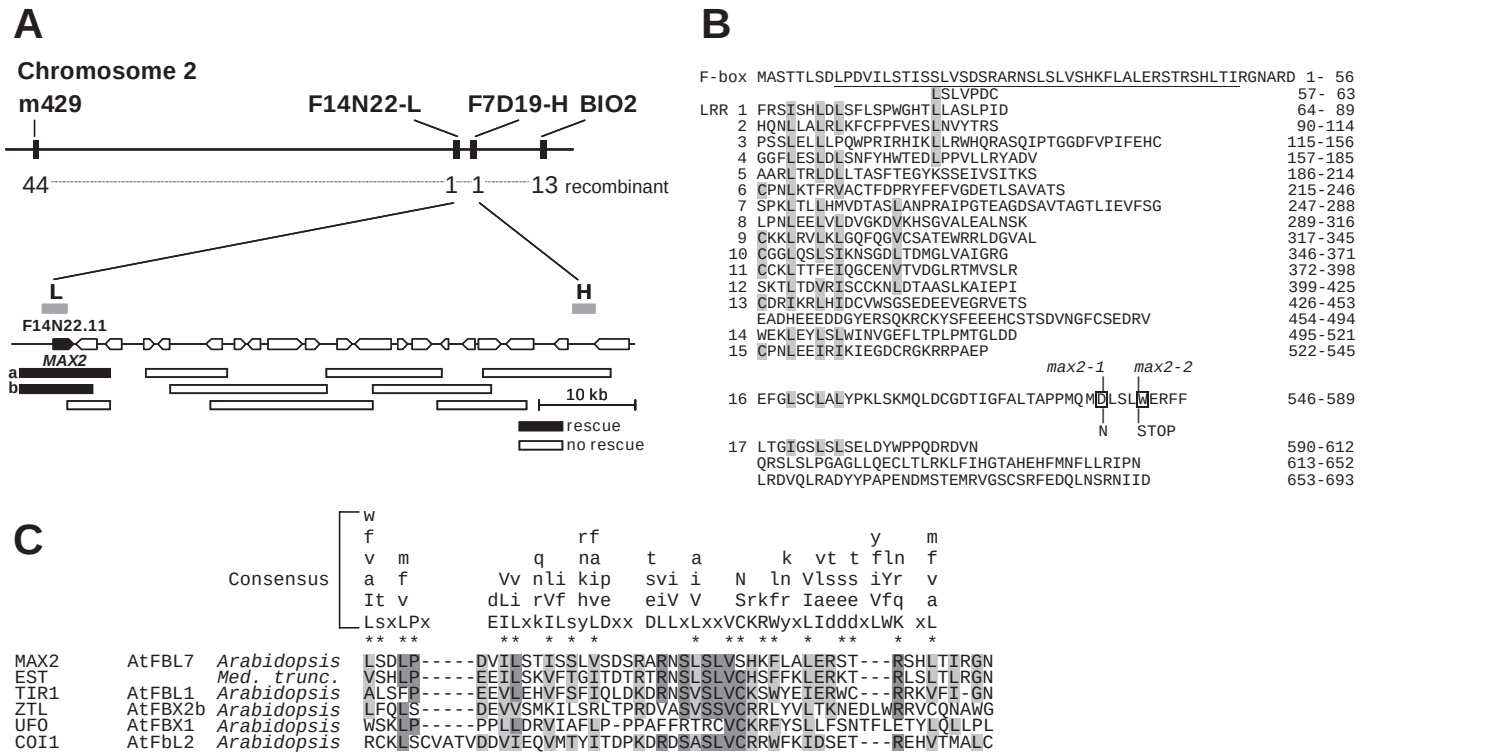

Fig. 9. *MAX2* encodes an F-box leucine-rich repeat protein. (A) Map-based cloning of the *MAX2* gene. (Top) The markers flanking *MAX2* that were used to screen for recombinants (m429, BIO2) and the closest flanking markers (F14N22-L, F7D19-H) that were located 57 kb apart on two overlapping BAC clones. The number of recombinant individuals, in a mapping population of 1300 plants, is given for each marker. (Bottom) The region between the closest flanking markers is enlarged to show the localisation of the PCR products for both markers (grey bars), the predicted gene structure (arrows), and the BAC subclones tested for mutant rescue (black and white bars). Mutant rescue by clones a and b identified F14N22.11 as the *MAX2* gene. (B) The predicted MAX2 protein sequence contains an F-box motif (underlined) and imperfect leucine-rich repeats (LRR). Positions with similar amino acids in several repeats are shaded. Amino acids affected by the *max2-1* and *max2-2* mutations are boxed and the predicted changes are shown. (C) Alignment of the predicted MAX2 F-box motif with a translation of the corresponding region found in two partial *Medicago truncatula* ESTs homologous to MAX2 (AL369069, BE325112), and with the F-boxes of other *Arabidopsis* proteins. A general F-box consensus (Patton et al., 1998) is given above the MAX2 sequence and the residues of MAX2 that match this consensus are marked (*). The second column shows the classification of predicted *Arabidopsis* F-box proteins used by Xiao and Jang (Xiao and Jang, 2000).

Branching control by *MAX2*

Our results suggest that an SCF^{MAX2} complex might act in the degradation of one or more proteins that activate axillary growth. An F-box dependent interaction between ORE9/MAX2 and ASK1, an *Arabidopsis* Skp1 family member, has already been demonstrated (Woo et al., 2001). To substantiate the model further, it will be necessary to show that MAX2 is part of SCF complexes in vivo. Identification of the protein(s) targeted for degradation will likely provide the key to understanding the exact role of MAX2 in branching control. Our mutant characterisation suggests that MAX2 might regulate axillary growth by repressing cell production rate in axillary shoot meristems. Therefore, an activator of cell cycle progression might be targeted by MAX2. The levels of many cell cycle regulatory proteins are controlled by ubiquitin-mediated proteolysis; for example, the yeast F-box LRR protein Grr1 targets G_1 cyclins Cln1/2 for degradation, thereby antagonising G_1 to S mitotic stage transition (Tyers and Jorgensen, 2000).

Targets of MAX2 may be identified by mutation. For example, mutations that stabilise a target protein by abolishing its interaction with MAX2 should be dominant and confer a *max2*-like branching phenotype. The *bushy* mutation in pea (Symons et al., 1999), and the *max5* mutation in *Arabidopsis* (K. v. d. S., unpublished) cause dominant loss of axillary growth control.

Conclusion

Our analysis of *MAX2* suggests a role for SCF-mediated protein degradation in the control of lateral shoot, leaf and hypocotyl growth. Further investigation of the role of *MAX2* and molecular cloning of other shoot branching regulators such as *MAX1*, should allow additional insight into how developmental and environmental signals are integrated to control shoot branching.

We thank Joanne Marrison, Audrey Sarps and Nicola Stock for help with gene mapping; Megan Stark for help with scanning EM and for photography; Jon Booker, Karen Halliday, and Karim Sorefan for helpful discussions; the University of York horticultural team for excellent plant care; the NASC, Nottingham, and ABRC, Ohio, for providing mutant and DNA stocks and Michael Schultze for critical reading of the manuscript. We gratefully acknowledge funding from

the Biotechnology and Biological Sciences Research Council of the UK and from the EU (Marie Curie Fellowship to K. v. d. S.).

REFERENCES

Bell, C. J. and Ecker, J. R. (1994). Assignment of 30 microsatellite loci to the linkage map of *Arabidopsis*. *Genomics* **19**, 137-144.

Beveridge, C. A. (2000). Long-distance signalling and a mutational analysis of branching in pea. *Plant Growth Regul.* **32**, 193-203.

Beveridge, C. A., Ross, J. J. and Murfet, I. C. (1996). Branching in pea. Action of genes *Rms3* and *Rms4*. *Plant Physiol.* **110**, 859-865.

Beveridge, C. A., Symons, G. M., Murfet, I. C., Ross, J. J. and Rameau, C. (1997). The *rms1* mutant of pea has elevated indole-3-acetic acid levels and reduced root-sap zeatin riboside content but increased branching controlled by graft-transmissible signal(s). *Plant Physiol.* **115**, 1251-1258.

Beveridge, C. A., Symons, G. M. and Turnbull, C. G. N. (2000). Auxin inhibition of decapitation-induced branching is dependent on graft-transmissible signals regulated by genes *Rms1* and *Rms2*. *Plant Physiol.* **123**, 689-697.

Chory, J. (1993). Out of darkness: mutants reveal pathways controlling light-regulated development in plants. *Trends Genet.* **9**, 167-172.

Clifford, R., Lee, M.-H., Nayak, S., Ohmachi, M., Giorgini, F. and Schedl, T. (2000). FOG-2, a novel F-box containing protein, associates with the GLD-1 RNA binding protein and directs male sex determination in the *C. elegans* hermaphrodite germline. *Development* **127**, 5265-5276.

Cline, M. G. (1991). Apical dominance. *Bot. Rev.* **57**, 318-358.

Cline, M. G. (1994). The role of hormones in apical dominance. New approaches to an old problem in plant development. *Physiol. Plant.* **90**, 230-237.

Clough, S. J. and Bent, A. F. (1998). Floral dip: a simplified method for *Agrobacterium*-mediated transformation of *Arabidopsis thaliana*. *Plant J.* **16**, 735-743.

Cockcroft, C. E., den Boer, B. G. W., Healy, J. M. S. and Murray, J. A. H. (2000). Cyclin D control of growth rate in plants. *Nature* **405**, 575-579.

Craig, K. L. and Tyers, M. (1999). The F-box: a new motif for ubiquitin dependent proteolysis in cell cycle regulation and signal transduction. *Prog. Biophys. Mol. Biol.* **72**, 299-328.

Dieterle, M., Zhou, Y.-C., Schäfer, E., Funk, M. and Kretsch, T. (2001). EID1, an F-box protein involved in phytochrome A-specific light signaling. *Genes Dev.* **15**, 939-944.

Doebley, J., Stec, A. and Gustus, C. (1995). *teosinte branched1* and the origin of maize: evidence for epistasis and the evolution of dominance. *Genetics* **141**, 333-346.

Doebley, J., Stec, A. and Hubbard, L. (1997). The evolution of apical dominance in maize. *Nature* **386**, 485-488.

Evans, M. M. S. and Barton, M. K. (1997). Genetics of angiosperm shoot apical meristem development. *Annu. Rev. Plant Physiol. Plant Mol. Biol.* **48**, 673-701.

Galan, J.-M., Wiederkehr, A., Seol, J. H., Haguenauer-Tsapis, R., Deshaies, R. J., Riezman, H. and Peter, M. (2001). Skp1p and the F-box protein Rcy1p form a non-SCF complex involved in recycling of the SNARE Snc1p in yeast. *Mol. Cell. Biol.* **21**, 3105-3117.

Grbić, V. and Bleecker, A. B. (1996). An altered body plan is conferred on *Arabidopsis* plants carrying dominant alleles of two genes. *Development* **122**, 2395-2403.

Hempel, F. D. and Feldman, L. J. (1994). Bi-directional inflorescence development in *Arabidopsis thaliana*: acropetal initiation of flowers and basipetal initiation of paraclades. *Planta* **192**, 276-286.

Jackson, P. K., Eldridge, A. G., Freed, E., Furstenthal, L., Hsu, J. Y., Kaiser, B. K. and Reimann, J. D. R. (2000). The lore of the RINGs: substrate recognition and catalysis by ubiquitin ligases. *Trends Cell Biol.* **10**, 429-439.

Kaplan, K. B., Hyman, A. A. and Sorger, P. K. (1997). Regulating the yeast kinetochore by ubiquitin-dependent degradation and Skp1p-mediated phosphorylation. *Cell* **91**, 491-500.

Kobe, B. and Deisenhofer, J. (1994). The leucine-rich repeat: a versatile binding motif. *Trends Biochem. Sci.* **19**, 415-421.

Konieczny, A. and Ausubel, F. M. (1993). A procedure for mapping *Arabidopsis* mutations using co-dominant ecotype-specific PCR-based markers. *Plant J.* **4**, 403-410.

Long, J. and Barton, M. K. (2000). Initiation of axillary and floral meristems in *Arabidopsis*. *Dev. Biol.* **218**, 341-353.

Millar, A. J., McGrath, R. B. and Chua, N.-H. (1994). Phytochrome phototransduction pathways. *Annu. Rev. Genet.* **28**, 325-349.

Napoli, C. A., Beveridge, C. A. and Snowden, K. C. (1999). Reevaluating concepts of apical dominance and the control of axillary bud outgrowth. *Curr. Top. Dev. Biol.* **44**, 127-169.

Nelson, D. C., Lasswell, J., Rogg, L. E., Cohen, M. A. and Bartel, B. (2000). *FKF1*, a clock-controlled gene that regulates the transition to flowering in *Arabidopsis*. *Cell* **101**, 331-340.

Oh, S. A., Park, J.-H., Lee, G. I., Paek, K. H., Park, S. K. and Nam, H. G. (1997). Identification of three genetic loci controlling leaf senescence in *Arabidopsis thaliana*. *Plant J.* **12**, 527-535.

Patton, E. E., Willems, A. R. and Tyers, M. (1998). Combinatorial control in ubiquitin-dependent proteolysis: don't Skp the F-box hypothesis. *Trends Genet.* **14**, 236-243.

Phillips, I. D. J. (1975). Apical dominance. *Annu. Rev. Plant Physiol.* **26**, 341-367.

Reintanz, B., Lehnen, M., Reichelt, M., Gershenzon, J., Kowalczyk, M., Sandberg, G., Godde, M., Uhl, R. and Palme, K. (2001). *bus*, a bushy Arabidopsis *CYP79F1* knockout mutant with abolished synthesis of short-chain aliphatic glucosinolates. *Plant Cell* **13**, 351-367.

Ruegger, M., Dewey, E., Gray, W. M., Hobbie, L., Turner, J. and Estelle, M. (1998). The TIR1 protein of *Arabidopsis* functions in auxin response and is related to human SKP2 and yeast Grr1p. *Genes Dev.* **12**, 198-207.

Russell, I. D., Grancell, A. S. and Sorger, P. K. (1999). The unstable F-box protein p58-Ctf13 forms the structural core of the CBF3 kinetochore complex. *J. Cell Biol.* **145**, 933-950.

Samach, A., Klenz, J. E., Kohalmi, S. E., Risseeuw, E., Haughn, G. W. and Crosby, W. L. (1999). The *UNUSUAL FLORAL ORGANS* gene of *Arabidopsis thaliana* is an F-box protein required for normal patterning and growth in the floral meristem. *Plant J.* **20**, 433-445.

Sambrook, J., Fritsch, E. F. and Maniatis, T. (1989). *Molecular Cloning: A Laboratory Manual*. Cold Spring Harbor, New York: Cold Spring Harbor Laboratory Press.

Somers, D. E., Schultz, T. F., Milnamow, M. and Kay, S. A. (2000). *ZEITLUPE* encodes a novel clock-associated PAS protein from *Arabidopsis*. *Cell* **101**, 319-329.

Stafstrom, J. P. and Sussex, I. M. (1992). Expression of a ribosomal protein gene in axillary buds of pea seedlings. *Plant Physiol.* **100**, 1494-1502.

Stirnberg, P., Chatfield, S. P. and Leyser, H. M. O. (1999). *AXR1* acts after lateral bud formation to inhibit lateral bud growth in Arabidopsis. *Plant Physiol.* **121**, 839-847.

Sussex, I. M. and Kerk, N. M. (2001). The evolution of plant architecture. *Curr. Opin. Plant Biol.* **4**, 33-37.

Symons, G. M., Murfet, I. C., Ross, J. J., Sherriff, L. J. and Warkentin, T. D. (1999). *bushy*, a dominant pea mutant characterised by short, thin stems, tiny leaves and a major reduction in apical dominance. *Physiol. Plant.* **107**, 346-352.

Tamas, I. A. (1995). Hormonal regulation of apical dominance. In *Plant hormones* (ed. P. J. Davies), pp. 572-597. Dordrecht: Kluwer Academic Publishers.

Tantikanjana, T., Yong, J. W. H., Letham, D. S., Griffith, M., Hussain, M., Ljung, K., Sandberg, G. and Sundaresan, V. (2001). Control of axillary bud initiation and shoot architecture in *Arabidopsis* through the *SUPERSHOOT* gene. *Genes Dev.* **15**, 1577-1588.

Tyers, M. and Jorgensen, P. (2000). Proteolysis and the cell cycle: with this RING I do thee destroy. *Curr. Opin. Genet. Dev.* **10**, 54-64.

Wilson, A. K., Pickett, F. B., Turner, J. C. and Estelle, M. (1990). A dominant mutation in *Arabidopsis* confers resistance to auxin, ethylene and abscisic acid. *Mol. Gen. Genet.* **222**, 377-383.

Woo, H. R., Chung, K. M., Park, J.-H., Oh, S. A., Ahn, T., Hong, S. H., Jang, S. K. and Nam, H. G. (2001). ORE9, an F-box protein that regulates leaf senescence in Arabidopsis. *Plant Cell* **13**, 1779-1790.

Xiao, W. and Jang, J.-C. (2000). F-box proteins in *Arabidopsis*. *Trends Plant Sci.* **5**, 454-457.

Xie, D.-X., Feys, B. F., James, S., Nieto-Rostro, M. and Turner, J. G. (1998). *COI1*: an *Arabidopsis* gene required for jasmonate-regulated defense and fertility. *Science* **280**, 1091-1094.

Zhao, D., Yu, Q., Chen, M. and Ma, H. (2001). The *ASK1* gene regulates B function gene expression in cooperation with *UFO* and *LEAFY* in *Arabidopsis*. *Development* **128**, 2735-2746.